DR. GUSTAVO ARRIZABALAGA (Orcid ID : 0000-0002-4445-0375)

TgDrpC, an atypical dynamin-related protein in *Toxoplasma gondii,* is associated with vesicular transport factors and parasite division

Running Title: Characterization of TgDrpC

Irene Heredero-Bermejo[1], Joseph M. Varberg[1], Robert Charvat[1], Kylie Jacobs[2], Tamila Garbuz[1], William J. Sullivan, Jr.[1,2*], and Gustavo Arrizabalaga[1,2*]

[1] Department of Pharmacology and Toxicology, Indiana University School of Medicine, Indianapolis, IN 46202

[2] Department of Microbiology and Immunology, Indiana University School of Medicine, Indianapolis, IN 46202

* Joint senior authorship: WJS and GA should be considered joint senior author.

Corresponding author: Gustavo Arrizabalaga. garrizab@iu.edu. Tel. +1 317-278-6355

Summary

Dynamin-related proteins (Drps) are involved in diverse processes such as organelle division and vesicle trafficking. The intracellular parasite *Toxoplasma gondii* possesses three distinct Drps. TgDrpC, whose function remains unresolved, is unusual in that it lacks a conserved GTPase Effector Domain, which is typically required for function. Here, we show that TgDrpC localizes to cytoplasmic puncta; however, in dividing parasites, TgDrpC redistributes to the growing edge of the daughter cells. By conditional knockdown, we determined that loss of TgDrpC stalls division and leads to rapid deterioration of multiple organelles and the IMC. We also show that TgDrpC interacts with proteins that exhibit homology to those involved in vesicle transport, including members of the adaptor

complex 2. Two of these proteins, a homolog of the adaptor protein 2 (AP-2) complex subunit alpha-1 and a homolog of the ezrin–radixin–moesin (ERM) family proteins, localize to puncta and associate with the daughter cells. Consistent with the association with vesicle transport proteins, re-distribution of TgDrpC to the IMC during division is dependent on post-Golgi trafficking. Together, these results support that TgDrpC contributes to vesicle trafficking and is critical for stability of parasite organelles and division.

Introduction

Toxoplasma gondii is an obligate intracellular protozoan parasite estimated to have infected one-third of the world population (Alvarado-Esquivel et al., 2016; Hill & Dubey, 2016; Pappas, Roussos, & Falagas, 2009). *Toxoplasma* is mainly acquired through consumption of undercooked meat from infected animals or by ingestion of environmental oocysts that are shed in the feces of infected felines, the definitive host. *Toxoplasma* is responsible for a large proportion of domestically acquired foodborne illnesses in United States, being the fourth leading cause of hospitalizations and the second leading cause of deaths ("Centers for Disease Control and Prevention. Burden of Foodborne Illness: Findings," ; Scallan et al., 2011). While *Toxoplasma* infections are typically asymptomatic in healthy individuals, they can have devastating consequences in immunosuppressed individuals and those infected congenitally (Dalimi & Abdoli, 2012). While the host immune response can control and eliminate the acute form (tachyzoite), the parasite can convert into a latent encysted form (bradyzoite) that establishes a chronic infection. Newly acquired infection or reactivation of latent cysts in immunodeficient individuals can lead to devastating tissue destruction and organ failure (Derouin & Pelloux, 2008; Khurana & Batra, 2016).

Toxoplasma employs a unique process of replication called endodyogeny, by which two daughter cells are formed inside a mature parasite (Blader, Coleman, Chen, & Gubbels, 2015). During endodyogeny, organelles must be segregated between the new daughter parasites (Nishi, Hu, Murray, & Roos, 2008; Radke et al., 2001). The cortical cytoskeleton complex, which includes a peripheral membrane system under the plasma membrane called the inner membrane complex (IMC), plays an important role during replication as it provides scaffold for the formation of the daughter parasites (B. Anderson-White et al., 2012; Blader et al., 2015). Early in division, *de novo* formation of the daughter IMC scaffold initiates, the apicoplast (a plastid-like organelle) and Golgi elongate, and the centrosome migrates from the apical to the posterior end of the nucleus. Next, Golgi division occurs, the centrosome duplicates, and karyokinesis and apicoplast division begins. Subsequently, the endoplasmatic reticulum (ER) enters the daugther scaffold and as the IMC elongates, the ER follows the nucleus and segregates into the daughter cells, a process that continues through the end of division. During this process, specialized secretory organelles (dense granules, micronemes, and rhoptries) are synthesized *de novo* from the Golgi within the forming daugther cells. Finally, the single mitochondrion from the mother enters each developing daughter parasite (Ovciarikova, Lemgruber, Stilger, Sullivan, & Sheiner, 2017).

In other eukaryotes, organelle division is often driven by self-assembling GTPases that form rings around the organelle and are involved in mechanically pinching membranes (Kuroiwa, 2010; McFadden & Ralph, 2003). Among these GTPases are classical mechanochemical dynamins and dynamin-related proteins (Drp) (Praefcke & McMahon, 2004). Drps have a GTPase effector domain (GED) that is required for the assembly of dynamin tetramers into the ring structure, and it is also involved in the stimulation of GTP hydrolysis after dynamin assembly (Fukushima, Brisch, Keegan, Bleazard, & Shaw, 2001; Muhlberg, Warnock, & Schmid, 1997). Drps are recruited by adaptor proteins associated with membrane organelles, which also participate in forming active fission complexes (Bui & Shaw, 2013). The formation of these complexes requires ATP, GTP, membrane lipids, actin, adaptor protein (AP) complexes or fission factors, among other components (Damke, 1996; Ugarte-Uribe, Muller, Otsuki, Nickel, & Garcia-Saez, 2014). In *Toxoplasma*, key proteins involved in the anterograde pathway regulating secretory organelle biogenesis have been identified (Venugopal et al., 2017), including dynamin-related protein B (DrpB), which associates with MIC2/M2AP and the AP-1 complex (Venugopal et al., 2017).

Eukaryotes possess a variable number of dynamin and dynamin-related proteins that are involved in organelle division. For example, the dynamin-related protein 1 (DRP1) in human cells (Smirnova, Griparic, Shurland, & van der Bliek, 2001) and the dynamin-related GTPase Dnm1p in yeast (Fukushima et al., 2001) mediate mitochondrial fission. The red algae, *Cyanidioschyzon merolae*, contains two dynamins (Dnm1 and Dnm2) that are involved in mitochondrial and plastid division, respectively (Kuroiwa, 2010). *Toxoplasma* possess three distinct Drp proteins: TgDrpA, TgDrpB, and TgDrpC (Breinich et al., 2009). Both TgDrpA and TgDrpB have all the conserved domains typical of Drps and have been shown to be required for apicoplast replication and secretory organelle biogenesis, respectively (Breinich et al., 2009; van Dooren et al., 2009). In contrast, TgDrpC (TGGT1_270690), whose function is not known, contains a GTPase domain but lacks the conserved GTPase Effector Domain (GED). The GED is typically required for efficient formation of dynamin oligomers and for stimulation of the GTPase domain activity (Chugh et al., 2006). As part of an effort to validate a novel strategy of gene silencing based on U1 snRNP, TgDrpC was shown to be essential, as parasites died following the induced gene disruption (Pieperhoff et al., 2015). The significant contribution of TgDrpC to parasite fitness was also confirmed in a genome-wide CRISPR screen (Sidik et al., 2016). While clearly essential for parasite viability, the biological function of TgDrpC remains unresolved.

To address this knowledge gap, we conducted a series of experiments aimed at characterizing TgDrpC during the replicative phase of *Toxoplasma*. Our findings revealed a dynamic redistribution of TgDrpC during parasite division, moving from cytosolic puncta in G0 to the pellicle of the daughter parasites during division. Additionally, using a conditional knockdown approach, we determined that loss of TgDrpC leads to rapid deterioration of the parasite, which includes mitochondrial fragmentation, and disruption of the apicoplast, and Golgi. Through immunoprecipitation studies, we establish that TgDrpC interacts with homologs of proteins associated with vesicle trafficking. Collectively, our results support a model that TgDrpC contributes to vesicular transport and is critical for parasite organelle integrity and division.

Results

TgDrpC exhibits a dynamic localization

To determine the localization of TgDrpC, we used a homologous recombination approach to generate a parasite line in which the endogenous protein includes a carboxyl terminal hemagglutinin (HA) epitope tag (Fig. 1A). Western blot assays of the resulting strain revealed an HA tagged protein migrating close to the expected size of 130 kD (Fig. 1B). Immunofluorescence assays of intracellular parasites expressing the tagged protein showed that TgDrpC signal had a mottled or punctate appearance distributed throughout the cytoplasm (Fig. 1C). TgDrpC puncta varied in intensity with several bright foci in each parasite (Fig. 1C arrows). On occasion, we observed that TgDrpC formed ring structures that appeared to coincide with daughter cell formation, as determined by diffused nuclear staining typical of dividing parasites (Fig. 1D). Indeed, this ring structure appeared to be localized to the growing edge of the daughter parasite pellicles, which was detected with antibodies against IMC3, a component of the inner membrane complex (IMC) (Chen et al., 2015) (Fig. 1E).

To further explore this localization pattern, we conducted immunofluorescence assays co-staining for TgDrpC and MORN1, a protein that is recruited to the apical complex of the nascent daughter cells early during parasite division and migrates with the growing daughter IMC through cytokinesis. During parasite division, MORN1 forms a ring structure located at the leading edge of the growing IMC, and this ring is required for constriction of the daughter IMC to complete cell division. TgDrpC co-localizes with MORN1-containing structures early during daughter cell formation and with the MORN1 ring during parasite division, remaining with this structure until the late stages of cytokinesis (Fig. 2).

In higher eukaryotic organisms, the dynamin-related protein Drp1 plays a key role in mitochondrial fission. As neither of the two Drp1 homologs from *Toxoplasma* studied to date, TgDrpA and TgDrpB, appear to be involved in mitochondrial fission (Breinich et al., 2009; van Dooren et al., 2009), it is plausible that TgDrpC is the dynamin-related protein that drives mitochondrial fission in *Toxoplasma*. Notwithstanding the fact that TgDrpC lacks several of the functional domains present in all Drps (Fig. 3A), we investigated whether it associates with the mitochondrion of the parasite. IFA of intracellular parasites stained for TgDrpC-HA and the mitochondrial marker F_1B ATPase showed that 58 ± 2% (Pearson's coefficient: 0.84 ± 0.1) of the larger foci of TgDrpC-HA co-localized to the mitochondrion as quantified using FIJI. Additionally, some TgDrpC foci localize to regions of the mitochondrion that appear to be constricted (Fig. 3B top row, arrowheads). In dividing parasites, the rings of TgDrpC appear to encircle mitochondrial material that remain contiguous between daughter parasites (Fig. 3B bottom row, arrows). Notably, association with the mitochondrion was not exclusive, as TgDrpC signal was evident at various other organelles including the Golgi, IMC and apicoplast (Fig. 3C).

Conditional knockdown of TgDrpC impairs parasite replication

While previous studies have shown TgDrpC to be essential for parasite viability (Pieperhoff et al., 2015), its function remains unresolved. We therefore generated a conditional knockdown of TgDrpC by fusing a destabilization domain (DD) to the C-terminus of the endogenous protein, along with an HA tag for tracking. The DD targets the fusion protein for degradation unless the stabilizing molecule Shield-1 (Shld1) is present in the growth medium (Banaszynski, Chen, Maynard-Smith, Ooi, &

Wandless, 2006; Herm-Gotz et al., 2007). When the TgDrpC-HA-DD expressing strain was maintained in the presence of Shld1, the fusion protein was expressed, albeit at lower levels than what is observed for the TgDrpC-HA strain (Fig. 4A). Residual TgDrpC-HA-DD protein was still detectable by Western blot 24 hours after Shld1 removal, but by 48 hours the protein levels were significantly reduced (89 ± 7% reduction, n=3, Fig. 4A). To more precisely determine the timeline of TgDrpC depletion, we grew parasites in the absence of Shld1 for 36, 42, and 48 hours (Fig. S1). No significant turnover of TgDrpC was detected until 42 hours (30 ± 2% reduction); 48 hours without Shld1 proved to be the time point among those tested showing maximum reduction of TgDrpC levels (Fig. S1).

We then evaluated parasite growth of the TgDrpC-HA-DD expressing line in the presence or absence of Shld1 for five and eight days. During this time, parasites typically undergo several cycles of invasion, replication, and cell lysis, forming areas of host cell clearance referred to as plaques. TgDrpC-HA-DD parasites did not form visible plaques in the absence of Shld1, even after eight days (Fig. 4B). Thus, conditional knockdown of TgDrpC reveals an essential role for this protein in parasite viability, consistent with findings previously reported for genetic ablation of TgDrpC (Pieperhoff et al., 2015).

To more closely examine this viability defect, we performed a parasite counting assay after 24 and 48 hours of growth in the presence or absence of Shld1 (Fig. 4C). At 24 hours, the distribution of different vacuole sizes was the same with or without Shld1, with most vacuoles having 4 or more parasites per vacuole (Fig. 4C). By 48 hours in the presence of Shld1, most vacuoles had only 1 or 2 parasites (Fig. 4C), indicating that between 24 and 48 hours, the parasites had undergone egress and re-invasion as expected. This is consistent with an increase in the number of vacuoles in the presence of Shld1 between 24 and 48 hours (Fig. 4D). By contrast, most vacuoles in TgDrpC-HA-DD cultures lacking Shld1 contained 32 or more parasites per vacuole (Fig. 4C), and no change in the number of vacuoles in culture between 24 and 48 hours (Fig. 4D). These results could be due to a subset of egressed vacuoles releasing parasites that are defective at reinvading new host cells. Thus, as levels of TgDrpC are reduced, parasites either stop dividing, no longer exit their host cell, or suffer an invasion defect upon egress.

The decreased viability seen after the loss of TgDrpC is accompanied by unusual tachyzoite morphology within the vacuoles. After 24 hours without Shld1, TgDrpC-HA-DD parasites appeared normal, but after 48 hours, a significant number of tachyzoites were swollen or vacuolated (Fig. 4E). Quantification of this phenotype indicated that only 43 ± 7% of vacuoles appeared normal in the absence of Shld1 compared to 90 ± 2% of vacuoles in Shld1. Furthermore, after 48 hours without Shld1, 36 ± 6% appeared swollen and 21 ± 2% vacuolated (Fig. 4F). Together, these results indicate that depletion of TgDrpC grossly disrupts parasite morphology, likely leading to death and resulting in reduced plaques.

Conditional knockdown of TgDrpC disrupts organelle maintenance and biogenesis
As dynamin-related proteins are often involved in organelle division, we evaluated the effects of TgDrpC depletion on the mitochondrion, apicoplast, and Golgi (Fig. 5A-C). After 48 hours without Shld1, all three organelles were abnormal in the swollen and vacuolated parasites, but appeared normal in unaffected vacuoles (Fig. 5). Fragmentation of mitochondria was detected in 74 ± 4% of swollen parasites 48 hours without Shld1 (Fig. 5D). Additionally, 48 ± 7% of swollen vacuoles

contained at least one parasite with lacking or disrupted apicoplast (Fig. 5B circled area, Fig. 5C and Fig. 5D). This phenotype was absent in those vacuoles that had normal appearance and was observed in 75 ± 9% of those that appeared vacuolated (Fig. 5D). Immunofluorescence images showed that the ATrx1 signal is disrupted; moreover, no apicoplast DNA signal is detectable by DAPI in those parasites (Fig. 5C), a phenotype consistent with loss of the apicoplast as previously reported by Lévêque et al. (Leveque et al., 2015). A similar pattern is observed with the Golgi in TgDrpC-HA-DD parasites grown without Shld1: 85 ± 7% of swollen vacuoles contained parasites in which the Golgi appeared as dispersed puncta in contrast to a solid structure typical of normal parasites (Fig. 5D). Therefore, the loss of TgDrpC leads to a rapid deterioration of the parasite, with an increase in the proportion of vacuolated parasites, and a catastrophic loss of organelle integrity.

As we observed a slight reduction in TgDrpC-HA-DD protein levels at 42 hours without Shld1, we looked for organelle and morphology alterations at this time point with the idea that we might observe partial phenotypes. Analysis of Golgi, apicoplast, and mitochondrion at 42 hours post Shld1 removal revealed similar patterns to those observed at 48 hours, with a majority of vacuoles that appeared aberrant having organellar defects (data not shown). Nonetheless, we were able to detect parasites within the same vacuole that differentially expressed TgDrpC (Fig. 6). Remarkably, the presence of TgDrpC correlates with the integrity of the mitochondrion and the Golgi: parasites expressing TgDrpC have a normal mitochondrion and Golgi, while those in the same vacuole but lacking TgDrpC have fragmented mitochondrion and disrupted Golgi (Fig. 6A-B, circled area). Thus, presence or absence of TgDrpC is tightly correlated with mitochondrial and Golgi integrity. In addition, parasites no longer expressing TgDrpC contained two apicoplasts, indicating a failure in parasite division (Fig. 6C, circled area).

IMC structure is altered in the absence of TgDrpC
Based on our observation that TgDrpC localizes to the daughter cells during parasite division, we inquired whether loss of TgDrpC affected the inner membrane complex during endodyogeny. Accordingly, we grew TgDrpC-HA-DD parasites without Shld1 for 42 hours and then visualized the IMC of both the mother and daughter cells. In the absence of Shld1, we consistently detected a larger proportion of parasites that exhibited aberrant IMC that was incomplete or disrupted compared to parasites grown in Shld1 (Fig. 7A, arrows). These alterations in IMC structure were detected in 32 ± 12% vacuoles grown without Shld1 for 42 hours (Fig. 7B). By contrast, this phenotype was detected in only 2 ± 1% of parasites in the presence of Shld1.

Interestingly, during our analysis of the IMC in TgDrpC-HA-DD parasites grown without Shld1, we observed that many of the parasites that lacked TgDrpC seemed to be in the process of dividing based on the presence of daughter cells as observed by staining for IMC (Fig. 7C). To determine whether this was a statistically significant phenomenon, we enumerated vacuoles in which parasites had daughter cells among those that were either TgDrpC positive or TgDrpC negative within the same culture. Of the vacuoles that had TgDrpC expression, 20 ± 2% had parasites in division, which is the normal proportion of parasites that are dividing at any time in an asynchronous *Toxoplasma* population (Radke et al., 2001). By contrast, 57 ± 6% of vacuoles negative for TgDrpC expression had parasites undergoing division (Fig. 7D). This phenomenon suggests that lack of TgDrpC might halt parasite division or leads to an accumulation of parasites undergoing endodyogeny, suggesting an association between this protein and parasite division.

TgDrpC interacts with proteins involved in vesicle transport

To provide more insight into the function of TgDrpC, we set out to identify the proteins with which it interacts. For this purpose, we performed three independent immunoprecipitation (IP) experiments from lysates of extracellular TgDrpC-HA parasites and used affinity purification and mass spectrometry to determine the identity of the interactors. As controls, we performed the same IP protocol with a non-specific mouse IgG and included a parasite strain that does not express an HA-tagged protein. Data from three independent IP experiments was analyzed using Significance Analysis of Interactome (SAINT) to assign confidence scores to protein-protein interactions (Choi et al., 2011; Teo et al., 2014). To increase confidence in the interacting candidates identified in the pull downs, we filtered the candidates using the following criteria: i) proteins for which no peptides were detected in either the non-specific IgG or in the non-HA expressing parasite strain controls; ii) proteins with peptides in all 3 IP assays and with more than 3 peptides in at least 2 of the assays; iii) SAINT score > 0.75 and fold-change (FC-B) > 2 (supplemental table S1). Implementation of these criteria resulted in a list of 15 putative interactors (Table 1), five of which shared homology to proteins involved in vesicle trafficking, such as adaptor protein 2 (AP-2) complex members (TGGT1_221940, TGGT1_272600, TGGT1_313450), intersectin-1 (TGGT1_227800), and ERM family protein (TGGT1_262150).

As Drps are known to be involved in vesicle transport, we focused our studies on TGGT1_272600 and TGGT1_262150, which show homology to the alpha subunit of the AP-2 complex and ERM family proteins, respectively. To determine the localization of these proteins, we used a homologous recombination approach to introduce a C-terminal myc epitope tag into the endogenous genes in the strain expressing TgDrpC-HA. Western blot assays of the resulting strains revealed myc-tagged proteins migrating close to the expected size of 183 kD for TGGT1_272600 and 89 kD for TGGT1_262150 (Fig. S2). For TGGT1_272600, we also detected additional bands of smaller size, which may be breakdown or cleavage products.

Immunofluorescence assays of intracellular parasites encoding the myc-tagged protein showed that TGGT1_272600 is low-abundant and localizes to puncta throughout the cytoplasm, which appear to concentrate within the daughter parasites during division (data not shown). Consistent with the IP, TGGT1_272600 co-localizes with bright puncta of TgDrpC and is recruited to the daughter parasites during division as observed for TgDrpC (data not shown). TGGT1_262150 also localized as puncta in the cytoplasm, and expression levels observed for this protein are much higher during parasite division (Fig. 8A), consistent with a previous report that this gene is cell cycle-regulated at the transcript level (Behnke et al., 2010). Furthermore, TGGT1_262150 co-localizes with IMC3 in the daughter parasites (Fig. 8A and 8B, arrows). However, both of these putative interactors are present in puncta that does not correspond to TgDrpC. This might be due to the heterogeneity of vesicles or multifunctionality of these factors. Nonetheless, the association or accumulation of both these proteins with daughter parasites support the idea that they, at least partially or temporarily, associate with TgDrpC. Finally, we immunoprecipitated TgDrpC-HA from the dual tagged strains and probed for the myc-tagged proteins. While we could not detect co-immunoprecipitation of TGGT1_272600, possibly due to its low abundance, TGGT1_262150 was detected in the HA immunoprecipitated but not in the controls, providing independent validation of this interaction (Fig. 8C).

TgDrpC localization is dependent on post-Golgi vesicle trafficking

Since our IP studies revealed a likely association between TgDrpC and proteins related to vesicle trafficking, we tested whether TgDrpC localization dynamics are dependent on post-Golgi trafficking. We treated intracellular parasites with 5µg/ml Brefeldin A (BFA), a Golgi-disrupting agent that inhibits protein transport from the endoplasmic reticulum to the Golgi apparatus (Harper et al., 2006). Incubating intracellular parasites with BFA for 30 minutes was sufficient to collapse the Golgi apparatus, which was detected by staining with the Golgi marker, TgSORTLR (Sloves et al., 2012) (Fig. 9A). While BFA treatment did not affect the dispersed puncta of TgDrpC, it disrupted the formation of TgDrpC rings in dividing parasites, which were identified based on nuclear morphology (Fig. 9B). As the nascent IMC remains intact in BFA treated parasites, this effect is not likely due to disruption of the daughter cells (Fig. 9C). Importantly, of those parasites that were dividing based on IMC staining, 2 ± 2% of parasites treated with BFA show TgDrpC rings compared to 98 ± 2% under normal conditions (Fig. 9D). Therefore, the presence of TgDrpC at the basal ring of daughter cells depends on post-Golgi trafficking.

Discussion

The opportunistic pathogen *Toxoplasma gondii* encodes for three dynamin-related proteins: DrpA, DrpB, and DrpC. TgDrpA and TgDrpB possess the conserved domains typical of Drps (Breinich et al., 2009; van Dooren et al., 2009). However, TgDrpC (TGGT1_270690) contains a GTPase domain but lacks the conserved GTPase Effector Domain (GED). Our studies using a conditional protein degradation system definitively establish the critical role of TgDrpC in parasite fitness. Parasites that express TgDrpC fused to a destabilization domain lose organellar integrity and likely die after stabilization compound Shield-1 (Shld1) is removed from the media. These parasites appear to divide and propagate normally in the absence of Shld1 for the first 36 hours but exhibit a significant disruption in growth at 48 hours. This timeline coincides with the protein degradation rate upon the removal of Shld1. The reason for the relative stability of the protein for the first 36 hours in the absence of Shld1 and the sudden reduction of protein levels between 36 and 48 hours is unclear. It is plausible that association of TgDrpC with stable protein complexes, vesicles or organellar membranes protects it from the proteasome. Regardless, the loss of TgDrpC elicits a rapid deterioration of the parasite integrity, with parasites becoming swollen and vacuolarized. In addition, all organelles examined, namely apicoplast, mitochondrion, IMC and Golgi, showed morphological disruptions. This catastrophic multiple organelle failure upon loss of TgDrpC is most evident in vacuoles that contain parasites differentially expressing TgDrpC (Fig. 7). Within these vacuoles, parasites still harboring TgDrpC possess normal organelle morphology while their intravacuolar neighbors lacking TgDrpC contain abnormal organelles.

Dynamin-related proteins in other eukaryotic systems are the key drivers of mitochondrial fission. As the other two Drp homologs found in *Toxoplasma* do not appear involved in mitochondrial division (Breinich et al., 2009; van Dooren et al., 2009), it was expected that TgDrpC would be the protein driving mitochondrial division during endodyogeny. However, TgDrpC lacks the domains known to be essential for the 'pinchase' function of dynamin-related proteins. Furthermore, a yeast two-hybrid screen using the *Toxoplasma* Fis1 as bait, which in other species recruits Drp to the mitochondria, did not reveal TgDrpC as a direct interactor (Jacobs and Arrizabalaga, unpublished

results); moreover, reciprocal immunoprecipitation of either TgDrpC or TgFis1 from a strain in which both proteins are epitope tagged did not reveal an interaction (data not shown). Interestingly, immunofluorescence assays showed that some of the large TgDrpC puncta are adjacent to areas where the mitochondrion appears constricted (Fig. 3B, top panels, arrowheads), but it remains unclear if this association has a functional consequence. We also see TgDrpC puncta associated with the Golgi and the IMC, suggesting the protein's function is not limited to a single organelle (Fig. 3C).

It is possible that the association of TgDrpC with the leading edge of the growing daughter IMC is reflective of the protein's function. In dividing parasites, TgDrpC always relocated from cytoplasm to ring like structures at the growing ends of the daughter buds. This localization parallels that of MORN1, a scaffolding protein essential in assembling the basal complex (Lorestani et al., 2012). Besides MORN1, the basal complex includes the centrin protein TgCen2 and the alveolin motif containing proteins IMC5, IMC8, IMC9, and IMC 13 (B. R. Anderson-White et al., 2011; Hu, 2008; Lorestani et al., 2012). In dividing parasites, the complex is assembled with the rest of the new cytoskeleton, forming a ring-like structure at the growing edge of the daughter cells. Towards the end of division, this ring constricts to cap the basal end of the new formed parasites to close the IMC and complete cytokinesis (Hu, 2008). The cap forms the mature basal complex, which is maintained and may play a structural role in tachyzoites (Lorestani et al., 2012). Thus, it is plausible that TgDrpC has a function in parasite division or in the formation or regulation of the basal body. Indeed, we noted an interesting association between loss of TgDrpC and parasite division. In cultures in which some parasites still had TgDrpC and some did not, we noted that nearly 60% of those without were undergoing endodyogeny. This contrasted with 20% of those that still had TgDrpC, which is approximately the usual proportion of parasites dividing in a normal asynchronous *Toxoplasma* culture (Radke et al., 2001). Thus, parasites without TgDrpC are more likely to be stuck in division. While it is possible that this is due to the particular timing of turnover, a likely explanation is that TgDrpC is needed for completion of the division cycle.

Functional insight about TgDrpC can also be ascertained from the protein composition of its interactome. After filtering for those interactors not seen in any of the controls and that have high statistical value we generated a list of 15 putative interactors, some of which are probably non-specific, like ribosomal proteins (TGGT1_216435, TGGT1_239330, and TGGT1_312960) and those predicted to be in the nucleus and involved in transcription (TGGT1_226240, TGGT1_227850, TGGT1_257070, and TGGT1_308890). One of the co-immunoprecipitated proteins is in rhoptries (TGGT1_294560). We focused on the five interactors that appeared to be involved in vesicle transport (TGGT1_272600, TGGT1_221940, TGGT1_227800, TGGT1_313450, and TGGT1_262150). We based this selection of the following: (i) TgDrpC localizes to puncta thorough the cytoplasm, which is reminiscent of vesicles; (ii) dynamins are involved in vesicle formation and transport; (iii) the TgDrpC relocalizes to the IMC during division, which is formed *de novo* early during parasite division (Agop-Nersesian et al., 2010; Tonkin, Beck, Bradley, & Boulanger, 2014) and involves clathrin-coated vesicles derived from the ER-Golgi secretory pathway (Harding & Meissner, 2014; Pieperhoff, Schmitt, Ferguson, & Meissner, 2013); and (iv), several factors that are involved in endocytosis and endosomal recycling, including Rab11A and Rab11B (Agop-Nersesian et al., 2010; Agop-Nersesian et al., 2009), contribute to the biogenesis of the IMC. Additionally, the link between TgDrpC and vesicle transport is supported by the results obtained from treating parasites with Brefeldin A (BFA), which prevents its redistribution to the ring structure associated with the IMC.

TgDrpC-interacting proteins TGGT_272600 and TGGT_221940 show homology to the alpha-subunit of the adaptor protein complex (AP-2). *Toxoplasma* has two adaptor complexes associated with clathrin, AP-1 and AP-2, that are specifically associated with the trans-Golgi network and the plasma membrane, respectively (Venugopal et al., 2017). Adaptor protein 2 (AP-2) complex is a heterotetramer consisting of two large adaptin subunits (α and β), a medium subunit (μ), and a small subunit (σ). This complex is involved in the formation of clathrin-coated vesicles during endocytosis. TGGT1_313450 showed homology to the clathrin adaptor complex small subunit and it is also expected to be involved in vesicle transport. TGGT1_227800 contains an EF domain that is found in proteins implicated in vesicle transport, and it also shows homology to intersectin-1 and dynamin associated protein 160. Related to intersectin-1, this is a Eps15 Homology (EH) domain-containing protein, which are known to play a role in clathrin-mediated endocytosis, and might also function in regulating signaling pathways by interacting with their EH domains. Furthermore, this protein binds to components of the endocytic complex, including dynamins (Adams, Thorn, Yamabhai, Kay, & O'Bryan, 2000). Finally, TGGT1_262150 showed homology to ERM family proteins, which are involved in linking the plasma membrane to the actin cytoskeleton. However, they are also involved in other functions such as endo/exocytosis, vesicle trafficking, or vesicle maturation (Chirivino et al., 2011; Jiang et al., 2014; Kvalvaag et al., 2013).

Among these five interactors, we tagged TGGT1_272600 (homolog of the adaptor protein 2 (AP-2) complex subunit alpha-1) and TGGT1_262150 (homolog of the ezrin–radixin–moesin (ERM) family proteins) and showed that both localize as cytoplasmic puncta like TgDrpC. Importantly, we observed that these putative TgDrpC interactors accumulate in the daughter cells during parasite division, as observed for TgDrpC. Nonetheless, we were not able to detect the interaction between TgDrpC and TGGT1_272600 in co-immunoprecipitation assays. It is possible that this is due to the low levels of TGGT1_272600 expression; alternatively, the majority of the protein may not coincide with the locale of TgDrpC. However, co-immunoprecipitation assays were able to confirm the interaction between TgDrpC and TGGT1_262150. The similar localization dynamics of TgDrpC and TGGT1_262150 during division support the idea that TgDrpC associates with vesicles that congregate at nascent daughter cells. We did not, however, observe a ring-like structure, indicating that they might be involved in general vesicle transport, while TgDrpC might either be associated in a subset of vesicles or be part of cargo delivered to the growing edge of the IMC. Furthermore, we confirmed that TGGT1_262150 co-localizes closely to the IMC in daughter parasites.

IMC formation initiates early and elongates through the end of division, forming a scaffold structure of flattened vesicles, intermediate filaments, and microtubules for new organelle assembly and segregation (Hu, 2008; Hu et al., 2002; Striepen, Jordan, Reiff, & van Dooren, 2007). The IMC of *Toxoplasma* is known to be constructed in part from clathrin-coated vesicles derived from the ER-Golgi secretory pathway (Harding & Meissner, 2014; Pieperhoff et al., 2013) and trafficking of vesicles to the daughter cell IMC is dependent on the small GTPase TgRab11b (Agop-Nersesian et al., 2010), TgALP1 (Harding & Meissner, 2014), TgStx6 (Harding & Meissner, 2014), and CHC1 (Pieperhoff et al., 2013). Studies performed with these proteins showed that their disruption led to a number of defects, including a block in IMC biogenesis, organellar defects, and replication arrest. Based on the current understanding of IMC formation and on our results, we hypothesize that TgDrpC may be part of this crucial process that plays an essential role in the structural integrity of the parasite. Whether TgDrpC is a driver of vesicle formation or fusion, or cargo with a different function, is a key question for future studies to address. It is tempting to speculate that TgDrpC plays a general role in vesicular

trafficking, as this could explain why its depletion leads to the rapid degeneration of multiple organelles as well as an inability to complete division. Whether all of the phenotypes are related or are the result of varied and independent roles is an exciting question to resolve.

Experimental procedures

Parasites culture and reagents
Parasites were maintained in culture by continuous passage through human foreskin fibroblasts (HFFs) grown to confluence in a humidified incubator at 37°C and 5% CO_2 concentration. The medium used was Dulbecco's Modified Eagle Medium supplemented with 10% fetal bovine serum (FBS), 50 µM penicillin-streptomycin and 2 mM L-glutamine. For selection of parasites expressing hypoxanthine-xanthine-guanine phosphoribosyl transferase (HXGPRT), medium was supplemented with 50 µg/ml mycophenolic acid and 50 µg/ml xanthine. For selection of dihydrofolate reductase (DHFR) expressing parasites, media contained 1 µM pyrimethamine. Shld1 was purchased from CheminPharma and dissolved in ethanol for a 500 mM stock solution. Brefeldin A was purchased from Fisher and dissolved in ethanol for a 5 mg/ml stock solution.

Generation of endogenously tagged parasite strains
To generate a strain in which the endogenous TgDrpC gene encoded a hemagglutinin (HA) epitope at the C terminus, a 1,549 base pair fragment of genomic DNA was amplified by PCR with primer set A (see Table S2 for sequence of all primers used in this study). This fragment was directionally cloned into the PacI site of the 3xHA-Lic-DHFR-TS plasmid (Huynh & Carruthers, 2009; LaFavers, Marquez-Nogueras, Coppens, Moreno, & Arrizabalaga, 2017) using In-Fusion Cloning (Clontech). The resulting vector was confirmed by restriction digestion and sequencing. Plasmid was linearized with EcoRV and transfected by electroporation into RH*ΔhxgprtΔku80* tachyzoites (Soldati & Boothroyd, 1993). To select for stable transfectants, parasites were maintained in the presence of 1 µM pyrimethamine and independent clones were established by limiting dilution.

A similar approach was used to introduce a Myc epitope tag at the carboxyl terminus of the putative TgDrpC interactors TGGT1_262150 and TGGT1_272600. To generate the tagging vectors for TGGT1_262150 and TGGT1_272600, we used primer sets B and C respectively and the resulting fragments were cloned into the PacI site of pLic-3xMYC-HXGPRT plasmids. The resulting vectors were transfected into either the RH*ΔhxgprtΔku80* parasite line (Huynh & Carruthers, 2009) or the TgDrpC HA expressing strain and selected for with 50 µg/ml mycophenolic acid with 50 µg/ml xanthine.

Generation of TgDrpC-HA-DD line
To generate a conditional knockdown strain, we employed a similar cloning strategy utilized to introduce the 3xHA epitope tag at the endogenous *TgDrpC* locus, but included a destabilization domain (DD) tag in the tagging construct cloned into the PacI site of the 2xHA-Lic-DHFR-TS. 100 µg of this tagging plasmid were linearized with EcoRV and transfected by electroporation into RH*ΔhxgprtΔku80* tachyzoites. Parasites were maintained in the presence of 1 µM pyrimethamine and independent clones were established by limiting dilution.

Immunofluorescence assays

For immunofluorescence assays (IFA), parasites were inoculated into HFF cells grown on 1.5 mm coverslips at a multiplicity of infection (MOI) of approximately 0.5 and incubated for 2 hours. Cultures were then washed to remove uninvaded parasites and incubated for 24 to 48 hours in absence or presence of 200 nM Shld1 prior to fixation with 4% paraformaldehyde in PBS for 15 minutes. Cultures were washed three times with PBS, blocked in PBS with 3% bovine serum albumin (BSA) for 30 minutes, and permeabilized with 3% BSA/PBS with 0.2% Triton X-100 (Thermo Scientific) for 30 minutes. Primary antibodies were incubated in 3% BSA/PBS + 0.2% Triton X-100 overnight at 4°C or for 90 minutes at room temperature. Then, coverslips were washed three times in PBS for 10 minutes and incubated with 3% BSA/PBS containing fluorophore conjugated secondary antibodies for 45 minutes at room temperature. Coverslips were then washed in PBS and mounted onto slides using DAPI containing Vectashield mounting media (Vector laboratories) (Varberg, LaFavers, Arrizabalaga, & Sullivan, 2018). Primary antibodies used were rabbit anti-HA (Cell Signalling Technology) at a 1:1,000 dilution, mouse anti-MYC (Cell Signalling Technology) at 1:1,000 dilution, rabbit anti-MORN1 (Gubbels, Vaishnava, Boot, Dubremetz, & Striepen, 2006), mouse anti-F1B-ATPase (Dr. Peter Bradley, unpublished) at a 1:2,000 dilution, mouse anti-ATrx1 (DeRocher et al., 2008) at a 1:2,000 dilution, rat anti-TgSORTLR (Sloves et al., 2012) at a 1:2,000 dilution, rat anti-IMC3 at a 1:2,000 dilution (Gubbels, Wieffer, & Striepen, 2004). Secondary antibodies used included goat anti-mouse and rabbit Alexa fluor 488/594 conjugated (Cell Signalling Technology) and were all used at a 1:2,000 dilution. Inspection of all samples was performed using a Nikon Eclipse E100080i microscope. Images were captured with a Hamamatsu C4742-95 charge-coupled device camera using NIS elements software.

Western blotting

Parasites were grown for 24 to 48 hours in HFFs, released from host cells by passage through a 27-gauge needle, and pelleted by centrifugation for 10 minutes at 1,000 x g. Pelleted parasites were washed once with cold PBS and then lysed in radio immunoprecipitation assay (RIPA) buffer plus protease and phosphatase inhibitors (Cell Signaling Technology) for 1 hour on ice. Lysate was sonicated twice for 10 seconds and centrifuged for 10 minutes at 13,000 RCF at 4°C and the supernatant was recovered. For time course experiments, protein concentration was determined by BCA Protein Assay (Pierce) and 20 μg of protein were run in 4%–20% gradient SDS-PAGE gel (Bio-Rad) and transferred into a nitrocellulose membrane using standard methodologies. Membranes were blocked in 5% milk in TBST for 20 minutes at room temperature, incubated overnight at 4°C with primary antibody in blocking buffer solution and with secondary antibody for 45 minutes at room temperature. Finally, blots were processed for imaging with SuperSignal™ West Femto Maximum Sensitivity Substrate (Thermo Fisher) and visualized with a FluorChem R imager (Bio-Techne) (Varberg et al., 2018). Primary antibodies used for western blots included rabbit anti-HA at a dilution of 1:1,000 (Cell Signaling Technologies), rabbit anti-MYC at a dilution of 1:1,000 (Cell Signaling Technologies), and mouse anti-SAG1 at a dilution of 1:2,000 (Genway). Secondary antibodies used include peroxidase-conjugated goat anti-mouse and anti-rabbit and were used at a 1:10,000 dilution.

Parasite growth assays

Growth was assessed by determining plaquing efficiency and growth rate (LaFavers et al., 2017). For doubling assays, 100,000 parasites were used to infect confluent HFF monolayers grown in 12-well tissue culture plates. Two-hours after infection, cultures were washed three times to remove parasites that did not attach or invade and the media was replaced with normal growth medium. At either 24 or 48 hours post infection, cells were fixed with methanol for 1 minute, dried, and stained using Differential Quik Stain kit (Polysciences, Inc). Number of parasites per vacuole was scored for at least 100 vacuoles for each well. For plaque assays, 500 parasites were used to infect a confluent HFF monolayer in 12-well plates. Infected cultures were incubated for 5 days and stained with Crystal Violet (Sigma Aldrich) to visualize plaques via imaging with a FluorChem R imager (Bio-Techne).

Co-immunoprecipitation (co-IP) assays

Naturally egressed parasites were collected by centrifugation, washed once with 1X PBS, suspended in 150 µl of IP Pierce buffer (Thermo Scientific) with protease and phosphatase inhibitor cocktail 100X (Cell Signaling Technology), and incubated for 1 hour on ice. After sonication, the lysate was centrifuged at 14,000 RPM for 10 minutes at 4°C. Supernatant was incubated with mouse IgG-conjugated magnetic beads (Cell Signaling Technology) for 1 hour at 4°C with slight rotation as a blocking step. Beads were spun down and kept for analysis and supernatant was incubated with either Pierce anti-HA or anti-MYC magnetic beads (Thermo Scientific). Beads were washed three times in 150 µl of IP Pierce buffer, twice in PBS, and once in dd-H$_2$O. Finally, beads were suspended in 40 µl of PBS. For detection of immunoprecipitated proteins by immunoblotting, the precipitated proteins were eluted off the magnetic beads by the addition of 40 µL 2x SDS-PAGE buffer containing 5% β-mercaptoethanol, boiled for 5 minutes at 95°C and analyzed by Western blot as described above.

For mass spectrometry analysis, samples were submitted to the Indiana University School of Medicine Proteomics Core facility for protein identification by mass spectrometry. The on-bead samples were first denatured in 8 M urea, reduced with 5 mM tris(2-carboxyethyl)phosphine, and alkylated with 10 mM chloroacetamide. Alkylated samples were then digested with 0.3 µg endoproteinase LysC (sequencing grade, Roche Diagnostics) overnight at 37°C. The samples were then diluted to a final concentration of 2M urea using 100 mM Tris-HCl, pH 8.5, and digested with 0.5 µg trypsin (Promega Gold) overnight at 37°C. Digested peptides were injected onto a 15 cm C18 column (PepMap, 3µm) on a Thermo Dionex UltiMate 3000 RSLCnano chromatography system, and eluted with a linear gradient from 3 to 40% acetonitrile (in water with 0.1% formic acid) over 120 min room temperature at a flow rate of 700 nL/min. Effluent was electrosprayed into a Orbitrap Velos Pro (Thermo-Fisher Scientific) mass spectrometer for analysis. Data analysis was performed using SEQUEST HT within Proteome Discoverer 2.1 (Thermo) and searched against the *Toxoplasma gondii* database (www.toxodb.org, TgondiiGT1_AnnotatedProteins version 29) with common contaminants using SEQUEST HT with an FDR of ≤1%. Results were imported into Scaffold 4 Q+ (Proteome Software) for additional analysis.

Statistical Analyses

All statistical analysis performed in this study were conducted using Prism (GraphPad v 7.0a). Statistical analysis of mass spectrometry results for the TgDrpC interactome was conducted using SAINTexpress (Choi et al., 2011; Teo et al., 2014).Co-localization analysis (coloc2 analysis) was performed with Fiji/ImageJ software to calculate Pearson's coefficient (Schindelin et al., 2012).

Author contributions

IHB, RC, JMV, WJS and GA conceived and designed the experiments. Results presented were generated by IHB (Figs. 1-9, Figs. S1-S2), JMV (Figs. 1, 2, 4, 5 and 9, Fig. S1), and RC (Fig. 3). KJ and TG generated the conditional knockout strains. IHB, JMV, WJS and GA analyzed all data presented. IHB, WJS and GA wrote the paper, with input from all authors.

References

Adams, A., Thorn, J. M., Yamabhai, M., Kay, B. K., & O'Bryan, J. P. (2000). Intersectin, an adaptor protein involved in clathrin-mediated endocytosis, activates mitogenic signaling pathways. *J Biol Chem, 275*(35), 27414-27420. doi:10.1074/jbc.M004810200

Agop-Nersesian, C., Egarter, S., Langsley, G., Foth, B. J., Ferguson, D. J., & Meissner, M. (2010). Biogenesis of the inner membrane complex is dependent on vesicular transport by the alveolate specific GTPase Rab11B. *PLoS Pathog, 6*(7), e1001029. doi:10.1371/journal.ppat.1001029

Agop-Nersesian, C., Naissant, B., Ben Rached, F., Rauch, M., Kretzschmar, A., Thiberge, S., . . . Langsley, G. (2009). Rab11A-controlled assembly of the inner membrane complex is required for completion of apicomplexan cytokinesis. *PLoS Pathog, 5*(1), e1000270. doi:10.1371/journal.ppat.1000270

Alvarado-Esquivel, C., Salcedo-Jaquez, M., Sanchez-Anguiano, L. F., Hernandez-Tinoco, J., Rabago-Sanchez, E., Beristain-Garcia, I., . . . Alvarado-Soto, E. (2016). Association Between Toxoplasma gondii Exposure and Heart Disease: A Case-Control Study. *J Clin Med Res, 8*(5), 402-409. doi:10.14740/jocmr2525w

Anderson-White, B., Beck, J. R., Chen, C. T., Meissner, M., Bradley, P. J., & Gubbels, M. J. (2012). Cytoskeleton assembly in *Toxoplasma gondii* cell division. *Int Rev Cell Mol Biol, 298*, 1-31. doi:10.1016/B978-0-12-394309-5.00001-8

Anderson-White, B. R., Ivey, F. D., Cheng, K., Szatanek, T., Lorestani, A., Beckers, C. J., . . . Gubbels, M. J. (2011). A family of intermediate filament-like proteins is sequentially assembled into the cytoskeleton of *Toxoplasma gondii*. *Cell Microbiol, 13*(1), 18-31. doi:10.1111/j.1462-

5822.2010.01514.x

Banaszynski, L. A., Chen, L. C., Maynard-Smith, L. A., Ooi, A. G., & Wandless, T. J. (2006). A rapid, reversible, and tunable method to regulate protein function in living cells using synthetic small molecules. *Cell, 126*(5), 995-1004. doi:10.1016/j.cell.2006.07.025

Behnke, M. S., Wootton, J. C., Lehmann, M. M., Radke, J. B., Lucas, O., Nawas, J., . . . White, M. W. (2010). Coordinated progression through two subtranscriptomes underlies the tachyzoite cycle of *Toxoplasma gondii*. *PLoS One, 5*(8), e12354. doi:10.1371/journal.pone.0012354

Blader, I. J., Coleman, B. I., Chen, C. T., & Gubbels, M. J. (2015). Lytic Cycle of *Toxoplasma gondii*: 15 Years Later. *Annu Rev Microbiol, 69*, 463-485. doi:10.1146/annurev-micro-091014-104100

Breinich, M. S., Ferguson, D. J., Foth, B. J., van Dooren, G. G., Lebrun, M., Quon, D. V., . . . Meissner, M. (2009). A dynamin is required for the biogenesis of secretory organelles in *Toxoplasma gondii*. *Curr Biol, 19*(4), 277-286. doi:10.1016/j.cub.2009.01.039

Bui, H. T., & Shaw, J. M. (2013). Dynamin assembly strategies and adaptor proteins in mitochondrial fission. *Curr Biol, 23*(19), R891-899. doi:10.1016/j.cub.2013.08.040

Centers for Disease Control and Prevention. Burden of Foodborne Illness: Findings.   Retrieved from https://www.cdc.gov/foodborneburden/2011-foodborne-estimates.html

Chen, A. L., Kim, E. W., Toh, J. Y., Vashisht, A. A., Rashoff, A. Q., Van, C., . . . Bradley, P. J. (2015). Novel components of the *Toxoplasma* inner membrane complex revealed by BioID. *MBio, 6*(1), e02357-02314. doi:10.1128/mBio.02357-14

Chirivino, D., Del Maestro, L., Formstecher, E., Hupe, P., Raposo, G., Louvard, D., & Arpin, M. (2011). The ERM proteins interact with the HOPS complex to regulate the maturation of endosomes. *Mol Biol Cell, 22*(3), 375-385. doi:10.1091/mbc.E10-09-0796

Choi, H., Larsen, B., Lin, Z. Y., Breitkreutz, A., Mellacheruvu, D., Fermin, D., . . . Nesvizhskii, A. I. (2011). SAINT: probabilistic scoring of affinity purification-mass spectrometry data. *Nat Methods, 8*(1), 70-73. doi:10.1038/nmeth.1541

Chugh, J., Chatterjee, A., Kumar, A., Mishra, R. K., Mittal, R., & Hosur, R. V. (2006). Structural characterization of the large soluble oligomers of the GTPase effector domain of dynamin. *FEBS J, 273*(2), 388-397. doi:10.1111/j.1742-4658.2005.05072.x

Dalimi, A., & Abdoli, A. (2012). Latent toxoplasmosis and human. *Iran J Parasitol, 7*(1), 1-17.

Damke, H. (1996). Dynamin and receptor-mediated endocytosis. *FEBS Lett, 389*(1), 48-51.

DeRocher, A. E., Coppens, I., Karnataki, A., Gilbert, L. A., Rome, M. E., Feagin, J. E., . . . Parsons, M. (2008). A thioredoxin family protein of the apicoplast periphery identifies abundant candidate transport vesicles in *Toxoplasma gondii*. *Eukaryot Cell, 7*(9), 1518-1529. doi:10.1128/EC.00081-08

Derouin, F., & Pelloux, H. (2008). Prevention of toxoplasmosis in transplant patients. *Clin Microbiol Infect, 14*(12), 1089-1101. doi:10.1111/j.1469-0691.2008.02091.x

Fukushima, N. H., Brisch, E., Keegan, B. R., Bleazard, W., & Shaw, J. M. (2001). The GTPase effector domain sequence of the Dnm1p GTPase regulates self-assembly and controls a rate-limiting step in mitochondrial fission. *Mol Biol Cell, 12*(9), 2756-2766.

Gubbels, M. J., Vaishnava, S., Boot, N., Dubremetz, J. F., & Striepen, B. (2006). A MORN-repeat protein is a dynamic component of the *Toxoplasma gondii* cell division apparatus. *J Cell Sci, 119*(Pt 11), 2236-2245. doi:10.1242/jcs.02949

Gubbels, M. J., Wieffer, M., & Striepen, B. (2004). Fluorescent protein tagging in *Toxoplasma gondii:* identification of a novel inner membrane complex component conserved among Apicomplexa.

Mol Biochem Parasitol, 137(1), 99-110. doi:10.1016/j.molbiopara.2004.05.007

Harding, C. R., & Meissner, M. (2014). The inner membrane complex through development of *Toxoplasma gondii* and *Plasmodium*. *Cell Microbiol, 16*(5), 632-641. doi:10.1111/cmi.12285

Harper, J. M., Huynh, M. H., Coppens, I., Parussini, F., Moreno, S., & Carruthers, V. B. (2006). A cleavable propeptide influences *Toxoplasma* infection by facilitating the trafficking and secretion of the TgMIC2-M2AP invasion complex. *Mol Biol Cell, 17*(10), 4551-4563. doi:10.1091/mbc.E06-01-0064

Herm-Gotz, A., Agop-Nersesian, C., Munter, S., Grimley, J. S., Wandless, T. J., Frischknecht, F., & Meissner, M. (2007). Rapid control of protein level in the apicomplexan *Toxoplasma gondii. Nat Methods, 4*(12), 1003-1005. doi:10.1038/nmeth1134

Hill, D. E., & Dubey, J. P. (2016). Toxoplasma gondii as a Parasite in Food: Analysis and Control. *Microbiol Spectr, 4*(4). doi:10.1128/microbiolspec.PFS-0011-2015

Hu, K. (2008). Organizational changes of the daughter basal complex during the parasite replication of *Toxoplasma gondii*. *PLoS Pathog, 4*(1), e10. doi:10.1371/journal.ppat.0040010

Hu, K., Mann, T., Striepen, B., Beckers, C. J., Roos, D. S., & Murray, J. M. (2002). Daughter cell assembly in the protozoan parasite *Toxoplasma gondii*. *Mol Biol Cell, 13*(2), 593-606. doi:10.1091/mbc.01-06-0309

Huynh, M. H., & Carruthers, V. B. (2009). Tagging of endogenous genes in a *Toxoplasma gondii* strain lacking Ku80. *Eukaryot Cell, 8*(4), 530-539. doi:10.1128/EC.00358-08

Jiang, L., Phang, J. M., Yu, J., Harrop, S. J., Sokolova, A. V., Duff, A. P., . . . Curmi, P. M. (2014). CLIC proteins, ezrin, radixin, moesin and the coupling of membranes to the actin cytoskeleton: a smoking gun? *Biochim Biophys Acta, 1838*(2), 643-657. doi:10.1016/j.bbamem.2013.05.025

Khurana, S., & Batra, N. (2016). Toxoplasmosis in organ transplant recipients: Evaluation, implication, and prevention. *Trop Parasitol, 6*(2), 123-128. doi:10.4103/2229-5070.190814

Kuroiwa, T. (2010). Mechanisms of organelle division and inheritance and their implications regarding the origin of eukaryotic cells. *Proc Jpn Acad Ser B Phys Biol Sci, 86*(5), 455-471.

Kvalvaag, A. S., Pust, S., Sundet, K. I., Engedal, N., Simm, R., & Sandvig, K. (2013). The ERM proteins ezrin and moesin regulate retrograde Shiga toxin transport. *Traffic, 14*(7), 839-852. doi:10.1111/tra.12077

LaFavers, K. A., Marquez-Nogueras, K. M., Coppens, I., Moreno, S. N. J., & Arrizabalaga, G. (2017). A novel dense granule protein, GRA41, regulates timing of egress and calcium sensitivity in *Toxoplasma gondii*. *Cell Microbiol, 19*(9). doi:10.1111/cmi.12749

Leveque, M. F., Berry, L., Cipriano, M. J., Nguyen, H. M., Striepen, B., & Besteiro, S. (2015). Autophagy-Related Protein ATG8 Has a Noncanonical Function for Apicoplast Inheritance in *Toxoplasma gondii*. *MBio, 6*(6), e01446-01415. doi:10.1128/mBio.01446-15

Lorestani, A., Ivey, F. D., Thirugnanam, S., Busby, M. A., Marth, G. T., Cheeseman, I. M., & Gubbels, M. J. (2012). Targeted proteomic dissection of *Toxoplasma* cytoskeleton sub-compartments using MORN1. *Cytoskeleton (Hoboken), 69*(12), 1069-1085. doi:10.1002/cm.21077

McFadden, G. I., & Ralph, S. A. (2003). Dynamin: the endosymbiosis ring of power? *Proc Natl Acad Sci U S A, 100*(7), 3557-3559. doi:10.1073/pnas.0831049100

Muhlberg, A. B., Warnock, D. E., & Schmid, S. L. (1997). Domain structure and intramolecular regulation of dynamin GTPase. *EMBO J, 16*(22), 6676-6683. doi:10.1093/emboj/16.22.6676

Nishi, M., Hu, K., Murray, J. M., & Roos, D. S. (2008). Organellar dynamics during the cell cycle of *Toxoplasma gondii*. *J Cell Sci, 121*(Pt 9), 1559-1568. doi:10.1242/jcs.021089

Ovciarikova, J., Lemgruber, L., Stilger, K. L., Sullivan, W. J., & Sheiner, L. (2017). Mitochondrial behaviour throughout the lytic cycle of *Toxoplasma gondii*. *Sci Rep, 7*, 42746. doi:10.1038/srep42746

Pappas, G., Roussos, N., & Falagas, M. E. (2009). Toxoplasmosis snapshots: global status of *Toxoplasma gondii* seroprevalence and implications for pregnancy and congenital toxoplasmosis. *Int J Parasitol, 39*(12), 1385-1394. doi:10.1016/j.ijpara.2009.04.003

Pieperhoff, M. S., Pall, G. S., Jimenez-Ruiz, E., Das, S., Melatti, C., Gow, M., . . . Meissner, M. (2015). Conditional U1 Gene Silencing in *Toxoplasma gondii*. *PLoS One, 10*(6), e0130356. doi:10.1371/journal.pone.0130356

Pieperhoff, M. S., Schmitt, M., Ferguson, D. J., & Meissner, M. (2013). The role of clathrin in post-Golgi trafficking in *Toxoplasma gondii*. *PLoS One, 8*(10), e77620. doi:10.1371/journal.pone.0077620

Praefcke, G. J., & McMahon, H. T. (2004). The dynamin superfamily: universal membrane tubulation and fission molecules? *Nat Rev Mol Cell Biol, 5*(2), 133-147. doi:10.1038/nrm1313

Radke, J. R., Striepen, B., Guerini, M. N., Jerome, M. E., Roos, D. S., & White, M. W. (2001). Defining the cell cycle for the tachyzoite stage of *Toxoplasma gondii*. *Mol Biochem Parasitol, 115*(2), 165-175.

Scallan, E., Hoekstra, R. M., Angulo, F. J., Tauxe, R. V., Widdowson, M. A., Roy, S. L., . . . Griffin, P. M. (2011). Foodborne illness acquired in the United States--major pathogens. *Emerg Infect Dis, 17*(1), 7-15. doi:10.3201/eid1701.P11101

Schindelin, J., Arganda-Carreras, I., Frise, E., Kaynig, V., Longair, M., Pietzsch, T., . . . Cardona, A. (2012). Fiji: an open-source platform for biological-image analysis. *Nat Methods, 9*(7), 676-682. doi:10.1038/nmeth.2019

Sidik, S. M., Huet, D., Ganesan, S. M., Huynh, M. H., Wang, T., Nasamu, A. S., . . . Lourido, S. (2016). A Genome-wide CRISPR Screen in Toxoplasma Identifies Essential Apicomplexan Genes. *Cell, 166*(6), 1423-1435 e1412. doi:10.1016/j.cell.2016.08.019

Sloves, P. J., Delhaye, S., Mouveaux, T., Werkmeister, E., Slomianny, C., Hovasse, A., . . . Tomavo, S. (2012). *Toxoplasma* sortilin-like receptor regulates protein transport and is essential for apical secretory organelle biogenesis and host infection. *Cell Host Microbe, 11*(5), 515-527. doi:10.1016/j.chom.2012.03.006

Smirnova, E., Griparic, L., Shurland, D. L., & van der Bliek, A. M. (2001). Dynamin-related protein Drp1 is required for mitochondrial division in mammalian cells. *Mol Biol Cell, 12*(8), 2245-2256.

Soldati, D., & Boothroyd, J. C. (1993). Transient transfection and expression in the obligate intracellular parasite *Toxoplasma gondii*. *Science, 260*(5106), 349-352.

Striepen, B., Jordan, C. N., Reiff, S., & van Dooren, G. G. (2007). Building the perfect parasite: cell division in apicomplexa. *PLoS Pathog, 3*(6), e78. doi:10.1371/journal.ppat.0030078

Teo, G., Liu, G., Zhang, J., Nesvizhskii, A. I., Gingras, A. C., & Choi, H. (2014). SAINTexpress: improvements and additional features in Significance Analysis of INTeractome software. *J Proteomics, 100*, 37-43. doi:10.1016/j.jprot.2013.10.023

Tonkin, M. L., Beck, J. R., Bradley, P. J., & Boulanger, M. J. (2014). The inner membrane complex sub-compartment proteins critical for replication of the apicomplexan parasite *Toxoplasma gondii* adopt a pleckstrin homology fold. *J Biol Chem, 289*(20), 13962-13973. doi:10.1074/jbc.M114.548891

Ugarte-Uribe, B., Muller, H. M., Otsuki, M., Nickel, W., & Garcia-Saez, A. J. (2014). Dynamin-related protein 1 (Drp1) promotes structural intermediates of membrane division. *J Biol Chem, 289*(44),

30645-30656. doi:10.1074/jbc.M114.575779

van Dooren, G. G., Reiff, S. B., Tomova, C., Meissner, M., Humbel, B. M., & Striepen, B. (2009). A novel dynamin-related protein has been recruited for apicoplast fission in *Toxoplasma gondii*. *Curr Biol, 19*(4), 267-276. doi:10.1016/j.cub.2008.12.048

Varberg, J. M., LaFavers, K. A., Arrizabalaga, G., & Sullivan, W. J., Jr. (2018). Characterization of Plasmodium Atg3-Atg8 Interaction Inhibitors Identifies Novel Alternative Mechanisms of Action in *Toxoplasma gondii*. *Antimicrob Agents Chemother, 62*(2). doi:10.1128/AAC.01489-17

Venugopal, K., Werkmeister, E., Barois, N., Saliou, J. M., Poncet, A., Huot, L., . . . Marion, S. (2017). Dual role of the *Toxoplasma gondii* clathrin adaptor AP1 in the sorting of rhoptry and microneme proteins and in parasite division. *PLoS Pathog, 13*(4), e1006331. doi:10.1371/journal.ppat.1006331

Table 1. List of putative TgDrpC interactors. Highlighted in yellow are those involved in vesicle transport. DrpC is highlighted in orange.

ID number	Annotation	Potential functional domains	Putative function
TGGT1_216435	hypothetical protein	Nop25 superfamily domain	Ribosome biogenesis
TGGT1_221940	adaptin n terminal region domain-containing protein	Adaptin N-terminal region domain (part of Adaptor protein complex AP-2, alpha)	Vesicle transport
TGGT1_226240	putative bud site selection protein	U1 like zinc finger domain	Nucleotide binding
TGGT1_227800	EF hand domain-containing protein	Eps15 homology (EH) domain (pair of EF hands found in proteins implicated in endocytosis, vesicle transport, and signaling); SMC domain Homology to Intersectin 1 and dynamin associated protein 160	Vesicle transport
TGGT1_227850	peptidyl-prolyl cis-trans isomerase, cyclophilin-type domain-containing protein	Cyclophilin with RRM domain	Chaperone, nucleotide binding
TGGT1_239330	ribosomal protein RPL37		Ribosome
TGGT1_257070	hypothetical protein	Med15 domain	Transcription
TGGT1_261450	hypothetical protein		
TGGT1_262150	kelch repeat containing protein	Kelch repeat domain (adaptor for ubiquitin ligases); ERM family protein (intermediates between actin cytoskeleton and plasma membrane); BTB domain (mediates dimerization)	Vesicle transport
TGGT1_270690	DrpC		
TGGT1_272600	adaptin c-terminal domain-containing protein	Adaptin C-terminal region domain (part of Adaptor protein complex AP-2, alpha); SMC domain	Vesicle transport
TGGT1_294560	rhoptry kinase family protein ROP37 (incomplete catalytic triad)		Signaling
TGGT1_305940	peptidyl-prolyl cis-trans isomerase, cyclophilin-type domain-containing protein	Cyclophilin with U-box domain	Chaperone, protein transport
TGGT1_308890	transcription elongation factor SPT6		Transcription
TGGT1_312960	hypothetical protein	Nop16 superfamily domain	Ribosome
TGGT1_313450	putative AP-2 complex subunit sigma-1	Clathrin adaptor complex small subunit	Vesicle transport

Figure legends

Figure 1. **TgDrpC localization.** A) Diagram of scheme used to introduce a triple hemagglutinin (3xHA) epitope tag into the endogenous TgDrpC gene. DHFR represents modified allele that confers resistance to pyrimethamine. B) Protein extracts from the parental or TgDrpC-HA expressing strain were analyzed by Western blot using anti-HA antibody. SAG1 was used as loading control. C-E) Intracellular TgDrpC-HA expressing parasites were stained with antibodies against HA. To detect dividing parasites, cultures were co-stained with either DAPI (blue in D) or IMC3 antibodies (green in E). The outlines in C delineates two individual parasites within the vacuole and arrows point at examples of bright puncta. Arrow in E point at the growing edge of daughter parasites. Scale bars = 3 μm.

Figure 2. **Redistribution of TgDrpC during parasite division.** Intracellular TgDrpC-HA expressing parasites were stained with anti-HA antibodies to detect TgDrpC (red) and with anti-MORN1 antibodies (green) to monitor parasites at different stages of division. Scale bar = 3 μm.

Figure 3. TgDrpC association with parasite organelles. A) Schematic diagram comparing the domain architecture of the three dynamin related proteins from *Toxoplasma* (TgDrpA, TgDrpB, and TgDrpC) with mammalian dynamin-1 and dynamin-1-like proteins. Domains indicated are GTPase, Central domain, Pleckstrin homology domain (PH), GTPase Effector Domain (GED), and WW-domain ligand protein domain (WWbp). B) Intracellular TgDrpC-HA expressing parasites were stained with anti-F1B ATPase to visualize the mitochondrion (red) and anti-HA antibodies to detect TgDrpC (green). Arrowheads point at the brightest dots that co-localize to the mitochondrion (top row) and arrows point at TgDrpC puncta enriched at constricted points along mitochondrion (bottom row). Scale bars = 2 μm. C) Parasites were stained for TgDrpC with anti-HA antibodies (red) and for the Golgi with anti-Sortilin (green, top row), the IMC with anti-IMC3 (green, middle row) or the apicoplast with anti-Atrx1 (green, bottom row). Circled areas show bright TgDrpC puncta that associate to the organelles analyzed. Scale bars = 6 μm.

Figure 4. Establishment and growth of parasite strain with conditional expression of TgDrpC. A) Western blots of extracts from parasites in which the endogenous TgDrpC was tagged with either HA or HA-DD grown for 24 or 48 hours in presence (+) or absence (-) of Shld1. Blots were probed with antibodies against HA to detect TgDrpC or against the surface antigen SAG1 as a loading control. B) Parasites expressing TgDrpC-HA-DD were allowed to grow for 5 and 8 days in the presence and absence of Shld1. Cultures were stained with Crystal Violet, which allows visualization of plaques (white areas) arising from parasites lysing their host cells (dark areas). C) Doubling assays quantifying the number of TgDrpC-HA-DD parasites per vacuole following 24 and 48 hours of growth in the presence or absence of Shld1 (n=3, ±SD). D) The total number of vacuoles of TgDrpC-HA-DD parasites at 24 and 48 hours with and without Shld1 was determined for 10 randomly selected fields of view. (n=3, ±SD) (***p<0.001). E) Phase image of TgDrpC-HA-DD parasites grown without Shld1 for 48 hours reveals aberrant vacuole structures. F) The distribution of vacuoles that appear normal, swollen, or vacuolated when parasites are grown with or without Shld1 for 48 hours (n=3, ±SD).

Figure 5. Organellar morphology in parasites lacking TgDrpC. A-C) Intracellular TgDrpC-HA-DD parasites were grown for 48 hours without Shld1 and stained with anti-F$_1$B-ATPase to detect mitochondria (A), with anti-ATrX1 to detect apicoplast (B), or with antibodies against the Sortilin-like

receptor (SORTLR) to detect Golgi (D). In A and B both normal (left) and abnormal right) vacuoles within the same culture are shown. In B, DNA is visualized with DAPI and circled area shows parasites that do not have an apicoplast based on lack of DAPI staining and diffuse ATrX1 staining. In A, B, and D, the left panels show vacuoles with normal morphology and the right panels show vacuoles that appear swollen, both within the same culture. C) Enlarged images of the areas circled in B. In parasites highlighted by arrows, there is no signal for DAPI staining and a diffused pattern of ATrX1. E) Graph shows the percentage of vacuoles within each category (i.e. normal, swollen, and vacuolated vacuoles) that have altered mitochondria (m), apicoplast (a), or Golgi (g), (n=3, ±SD). Scale bars = 6 μm.
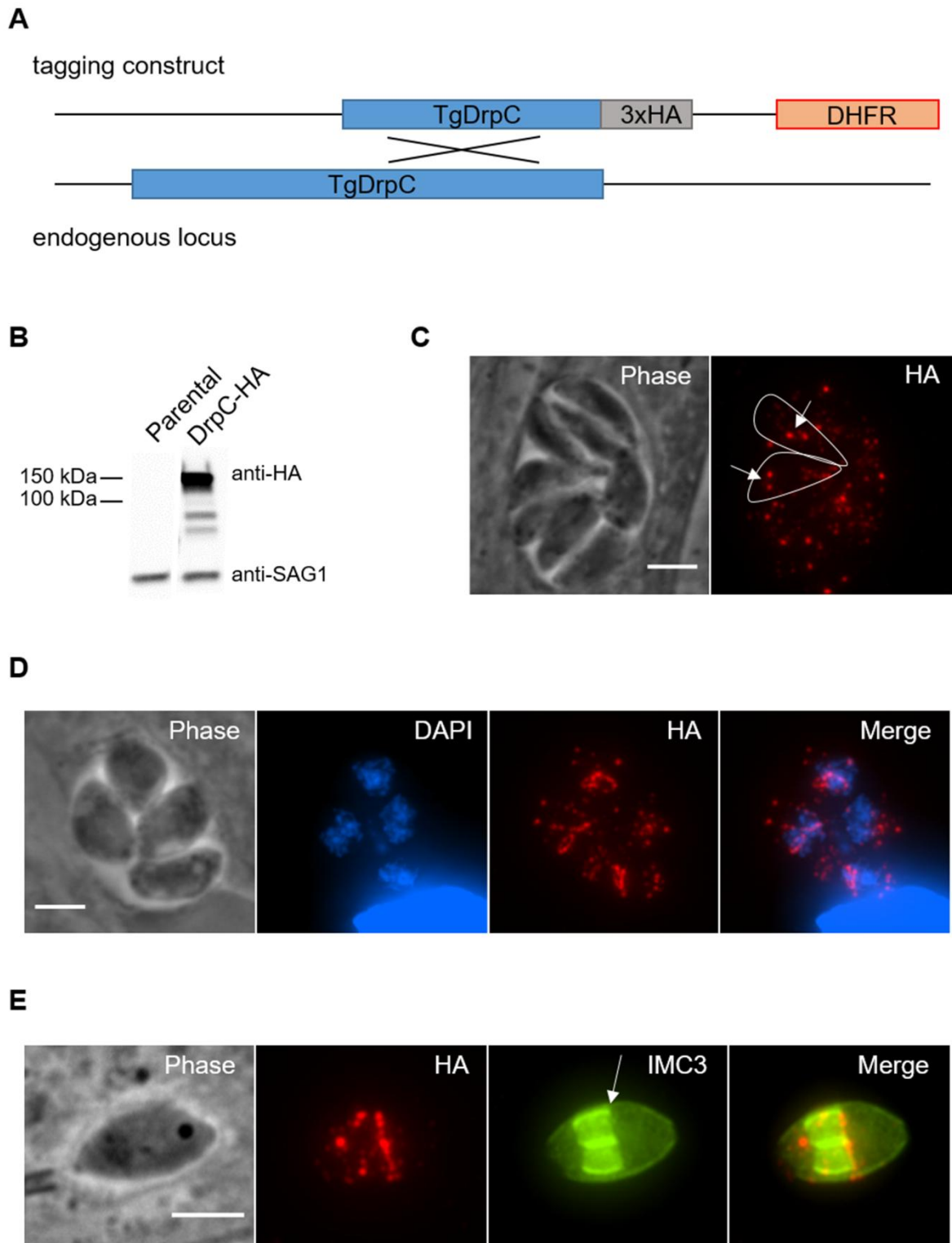
Figure 6. TgDrpC and organellar morphology. A-C) Intracellular TgDrpC-HA-DD parasites grown without Shld1 for 42 hours were stained with HA to detect TgDrpC and with anti-F1B-ATPase to detect mitochondria (A), with antibodies against the Sortilin-like receptor (SORTLR) to detect Golgi (B) or with anti-ATrX1 to detect apicoplast (C). In A, circles highlight areas within a single vacuole in which parasites with and without TgDrpC are detected, in B circles highlight areas with TDrpC and normal Golgi, and in D circles highlight areas without TgDrpC. Arrows indicate normal mitochondria. Scale bar = 6 μm.
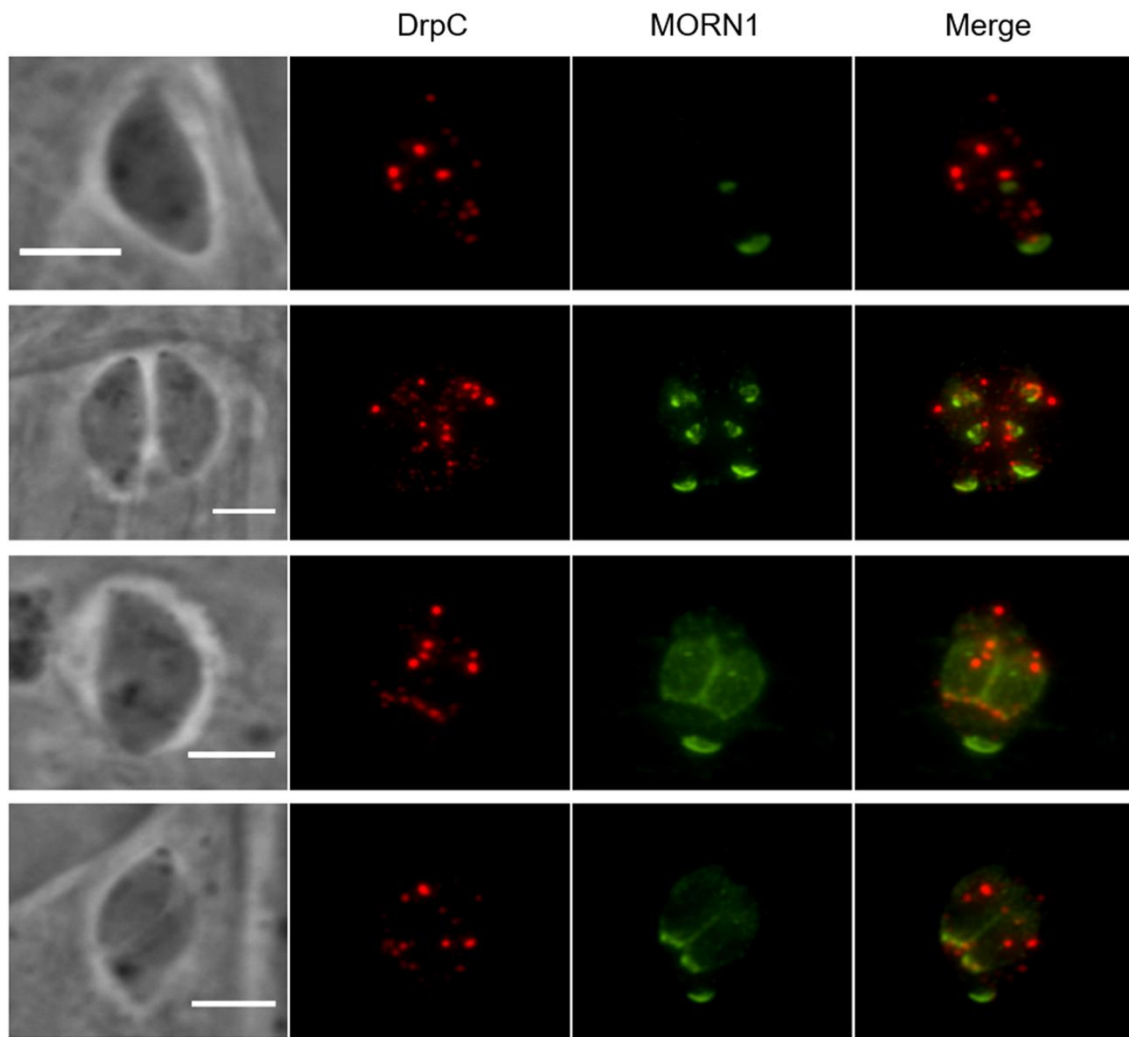
Figure 7. Inner membrane complex formation and parasite division in absence of TgDrpC. A) Immunofluorescence analysis of DrpC-HA-DD parasites grown for 42 hours in absence of Shld1. Anti-IMC3 antibody was used to detect the inner membrane complex. Images of parasites with either normal or altered IMC are shown. Arrows indicate IMC alterations. Scale bar = 3 μm. B) Percentage of vacuoles with altered IMC structure at 42 hours with or without Shld1. (n=3, ±SD) (*p<0.001). C) Intracellular DrpC-HA-DD expressing parasites grown for 42 hours without Shld1 were stained with antibodies against HA to detect TgDrpC (red). To detect dividing parasites, samples were co-stained with either DAPI (blue) and IMC3 antibodies (green). Circled area indicates dividing parasites. Scale bar = 6 μm. D) Percentage of vacuoles with or without DrpC signal in which parasites were dividing at 42 hours without Shld1. (n=3, ±SD) (*p<0.001).
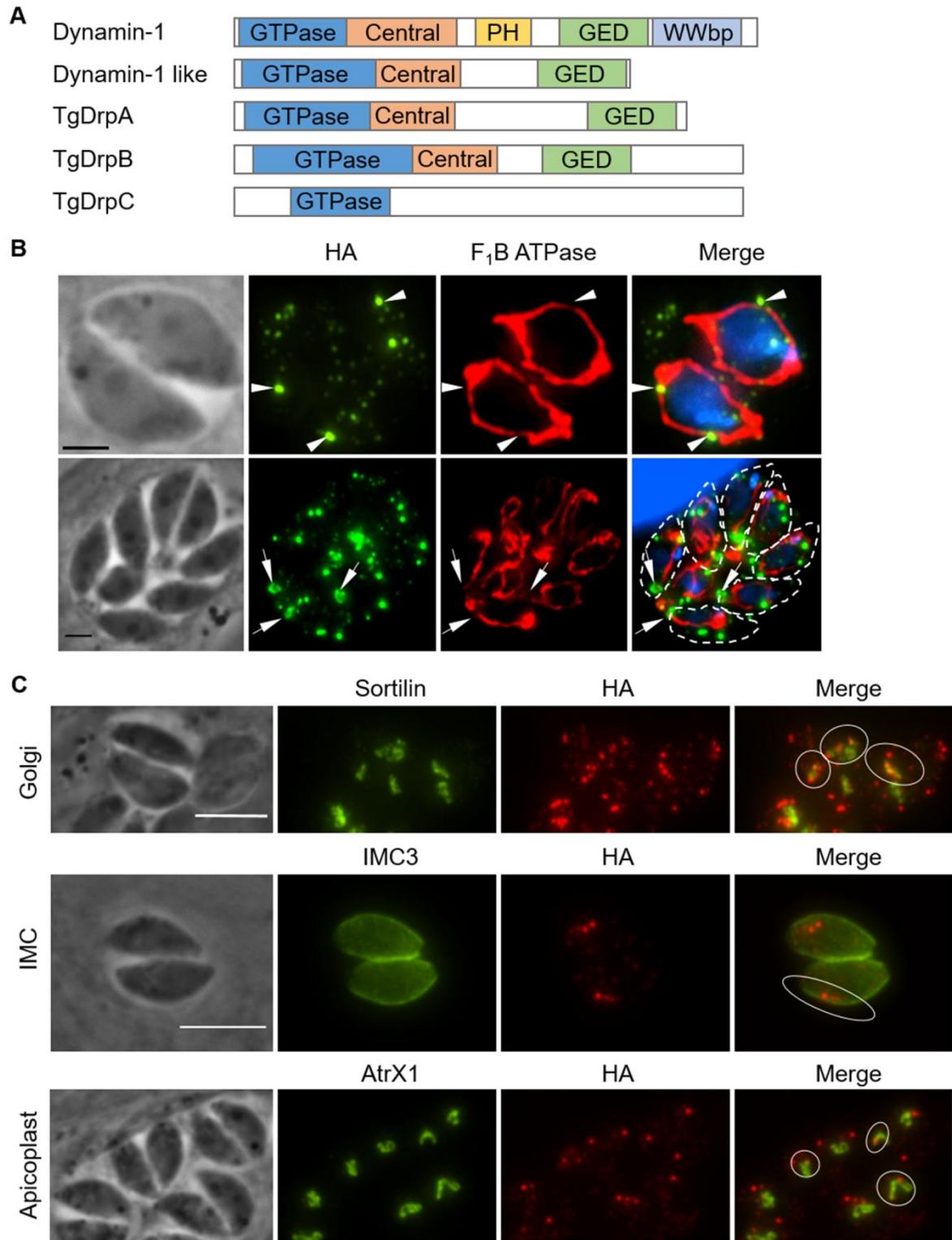
Figure 8. **Probing interaction between TgDrpC and homolog of ERM family proteins.** A myc epitope tag was added to the endogenous gene TGGT1_262150 in the parasite strain expressing TgDrpC-HA. A) Dually tagged strain stained with anti-myc (green) and IMC3 (red) antibodies to detect TGGT1_262150 and TgDrpC. Bottom row shows dividing parasites. Boxed area was enlarged to show co-localization in the overlay on the left. Arrows indicate co-localization of TGGT1_262150 and IMC3. Scale bar = 3 μm (top row), 6 μm (bottom row). B) Dually tagged strain stained with anti-myc (green) and anti-HA (red) antibodies to detect TGGT1_262150 and TgDrpC. Bottom row shows dividing parasites. Arrows indicate co-localization of TGGT1_262150 and TgDrpC. Circled area shows localization to the TgDrpC-containing ring structure and protein recruitment to the daughter parasites (arrow point to the TgDrpC ring structure). Scale bar = 3 μm. C) Immunoblot showing reciprocal co-immunoprecipitation of TgDrpC-HA and TGGT1_262150-MYC using HA magnetic beads and IgG as a negative control.

Figure 9. Localization of TgDrpC in Brefeldin A treated parasites. A) Disruption of the Golgi apparatus in intracellular tachyzoites after 5μg/ml Brefeldin A (BFA) treatment for 30 minutes was confirmed by staining with antibodies against sortilin-like receptor (SORTLR). Control tachyzoites were incubated with ethanol (EtOH), which was used as vehicle. Scale bar = 3 μm B) Intracellular

parasites were treated with EtOH (control) or 5µg/ml BFA for 30 min and stained IMC3 (green) to detect dividing parasites and with HA to detect TgDrpC (red). Both dividing and non-dividing parasites are shown. Scale bar = 3 µm C) Graph shows the percentage of vacuoles with TgDrpC ring structures among those that are dividing in cultures treated with BFA or ethanol as control. (n=3, ±SD) (*p < 0.0001).

A

tagging construct

endogenous locus

B

C

D

E

A

24 hrs   48 hrs

DrpC: HA   HA-DD   HA   HA-DD

Shld1: + -   + -   + -   + -

anti-HA

anti-SAG1

B   DrpC-HA-DD

5 days   8 days

+ Shld1

- Shld1

C

D

E

Swollen

Vacuolated

Normal

F

Figure 5

A
Mitochondria | DrpC | Merge

B
DrpC | Golgi | Merge

C
DrpC | Apicoplast | Merge

A

Normal | Altered | Altered | Altered

Phase

IMC

+ Shld1 | − Shld1

B

C

Phase | DAPI | HA | IMC3 | Merge

D

A

Non dividing

Dividing

TGGT1_262150   IMC

B

Non dividing

Dividing

TGGT1_262150   DrpC   Merge

C

Probed with anti-HA

input   flow through   elution
         IgG   HA   IgG   HA

150 kD —
100 kD —
75 kD —

Probed with anti-MYC

input   flow through   elution
         IgG   HA   IgG   HA

100 kD —
75 kD —